10
Conclusion

10.1 Scope

We have introduced the new critical state concept among older concepts of classical soil mechanics, but it would be wrong to leave any impression at the end of this book that the new concept merely rejuvenates the classical calculations. In this brief conclusion we concentrate only on the new concept of critical states and try to illustrate in a compact manner the new insight into the mechanical behaviour of soil under three headings:
§10.2 We acquire a new basis for engineering judgement of the state of ground and the consequences of proposed works.
§10.3 We can review existing tests and devise new ones.
§10.4 We can initiate new research into soil deformation and flow.

10.2 Granta-gravel Reviewed

Let us review the Granta-gravel model in Fig. 10.1(a), where we plot six curved λ-lines at equal spacings lettered VV, AA, BB, CC, DD, and EE on the (v, p) plane. The double line CC represents the *critical states* and the line VV represents *virgin isotropic compression* of Granta-gravel. Between VV and CC we have *wet states* of soil in which it consolidates in Terzaghi's manner, and AA and BB are typical curves of anisotropic compression. Under applied loading the *wet* soil flows and develops positive pore-pressures or drains and hardens; the whole soil body tends to deform plastically, and hence, the typical drainage paths are long and the *undrained* problem occurs resulting in *immediate* limiting equilibrium problems which involve calculations with $k = c_u$ and $\rho = 0$.

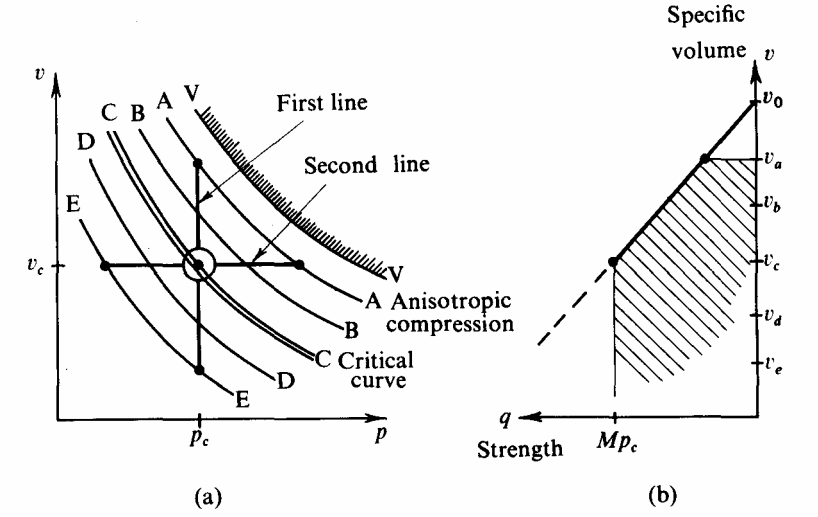

Fig. 10.1 Review of Granta-gravel

In contrast, the curves DD and EE are in the *dry states* of soil in which it ruptures and slips in Coulomb's manner as a rubble of blocks. Each thin slip zone has a short drainage path and the *drained* problem occurs resulting in *long-term* limiting equilibrium

problems which involve calculations with $k = 0$ and ρ at a value consistent with the critical states.

Across the Fig. 10.1(a) we draw two bold lines that correspond to two interesting engineering problems. The first line is at *constant effective spherical pressure* p_c and it intersects the λ-lines at specific volumes $v_a, v_b, v_c, v_d,$ and v_e. The second line is at *constant specific volume* v_c and it intersects the λ-lines at $p_a, p_b, p_c, p_d,$ and p_e. In Fig. 10.1(b) we plot the stable state boundary curve that corresponds to the first line; what does the figure imply?

We can think of $v_a, v_b, v_c, v_d,$ and v_e as being the alternative specific volumes to which a layer of saturated remoulded Granta-gravel can be compacted by alternative increasingly costly *compaction* operations. Suppose that the layer will eventually form part of an *embankment* in which it will be under some particular value of effective spherical pressure p_c. We consider what benefit is to be gained from increased compaction, and Fig. 10.1(b) shows that from v_a to v_b to v_c there is a steady increase in strength q, but from v_c to v_d to v_e further compaction is wasted. For, while individual blocks might have increasing strengths (near the dotted line in Fig. 10.1(b)), the engineering design of the embankment would have to proceed on the assumption that the blocks would be ruptured in the long-term problem and that the relevant strength parameter was Mp_c. There is no gain in *guaranteed* strength with increased compaction beyond the critical state.

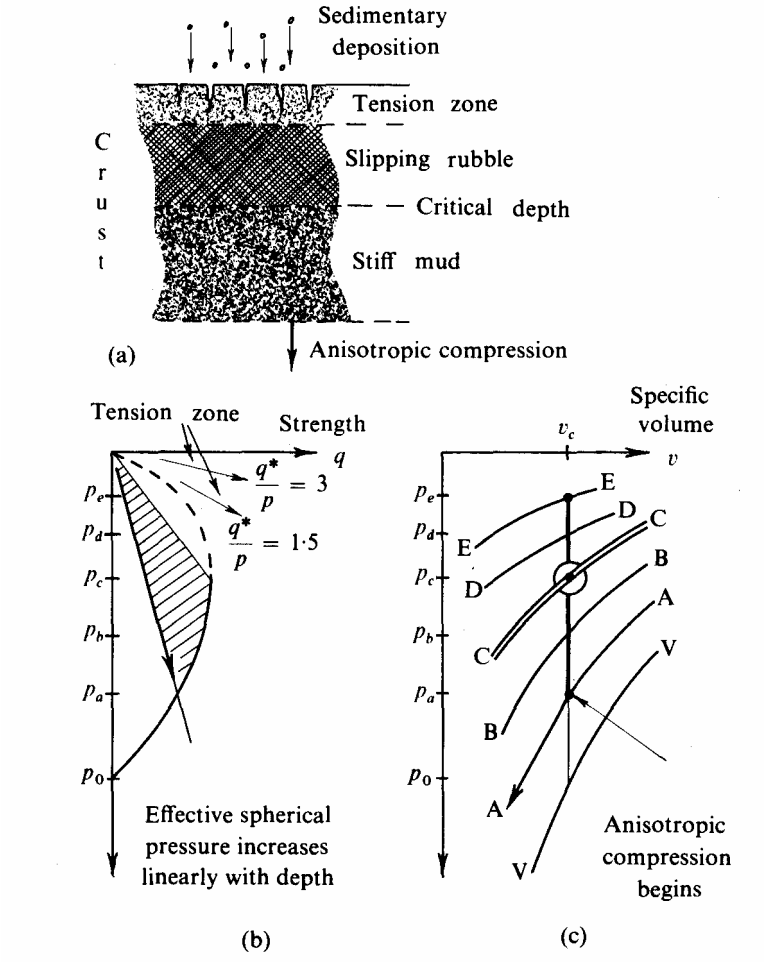

Fig. 10.2 The Crust of a Sedimentary Deposit

The second line in Fig. 10.1(a) at *constant specific volume* leads in Fig. 10.2 to three diagrams. Figure 10.2(c) is identical to part of Fig. 10.1(a) rotated through 90°, and 10.2(b) shows the stable state boundary curve that corresponds to the second line; what do these figures imply?

Figure 10.2(a) shows a *sedimentary deposit* of saturated remoulded (isotropic and homogeneous) Granta-gravel with particles falling on to the surface and forming a deposit of *constant* specific volume v_c. As the deposit builds up so the effective spherical pressure on any layer of material steadily increases; we plot the axis of p increasing downwards with depth in the deposit. In Fig. 10.2(c) the deposit of Granta-gravel remains rigid at specific volume of v_c to a depth at which anisotropic compression (under K_0 conditions) occurs under effective spherical pressure p_a. The sediment above that depth forms a sort of *crust:* we can ask what would be the response of material at various depths to any disturbance. During any deformation the Granta-gravel will require a sufficient supply of power to satisfy the basic equation, (5.19),

$$\frac{p\dot{v}}{v} + q\dot{\varepsilon} = Mp|\dot{\varepsilon}|.$$

At a depth where the effective spherical pressure is p_a, there is enough power available from plastic collapse of volume to satisfy eq. (5.19) without any need for a large additional deviatoric stress to cause the disturbance. At a smaller depth, where the effective spherical pressure is only p_b, there is less power available from plastic collapse of volume and more deviatoric stress would be needed to cause the disturbance: that is to say, the material gains strength *higher* in the crust. At a critical depth where the effective spherical pressure is p_c, there is no plastic collapse of volume, and the crust has its greatest strength. Above the critical depth we expect the material to deform as a rubble of slipping blocks in Coulomb's manner.

A small digression is appropriate about the possible tension zones in Fig. 10.2(b). Introducing $\sigma'_1 > \sigma'_2 = \sigma'_3 = 0$ into the generalized stress parameters briefly suggested in §8.2

$$p^* = \frac{\sigma'_1 + \sigma'_2 + \sigma'_3}{3}, \qquad q^* = \left| \left(\frac{(\sigma'_2 - \sigma'_3)^2 + (\sigma'_3 - \sigma'_1)^2 + (\sigma'_1 - \sigma'_2)^2}{2} \right)^{\frac{1}{2}} \right|$$

we find $p^* = \sigma'_1/3, q^* = \sigma'_1,$ and $q^*/p^* = 3,$ which gives one radial line shown in Fig. 10.2(b). Another radial line with $q^*/p^* = 1.5$ corresponds with $\sigma'_1 = \sigma'_2 > \sigma'_3 = 0$ where we find $p^* = (2\sigma'_1/3)$ and $q^* = \sigma'_1.$ These two lines indicate the range of values $1.5 < (q^*/p^*) < 3$ in which one or more of the principal effective stress components $(\sigma'_1, \sigma'_2, \sigma'_3)$ becomes zero. In that zone we can have stressed soil bodies with one stress-free face, which implies that slight tension cracks or local pitting of the surface of the sedimentary deposit could occur.

Finally, moving down through the deposit in Fig. 10.2(a) we have first a shallow zone of possible tension cracks above a zone of slipping rubble; below a critical depth (which is a function of v_c) the material would behave as a stiff mud, readily expelling water under small deviatoric stress, and finally all material below the depth associated with p_a is in some state of anisotropic compression at a specific volume less than v_c. A Granta-gravel sediment would not experience this anisotropic compression until it was overlain by a thickness of crust formed by subsequent sediment.

In Fig. 10.1(b) we have considered the value of compaction to alternative specific volumes, and in Fig. 10.2 the state of a sedimentary deposit. Clearly with the critical state concept we have acquired a new basis for engineering judgement of the state of ground and the consequences of proposed works.

10.3 Test Equipment

We have seen (6.9) that the plasticity index corresponds to a critical state property that could be measured with more precision by other tests, such as indentation by a falling cone. Our discussion of the refined axial-test apparatus of §7.1 shows that an apparatus which attains this high standard can give data of altogether greater value than the conventional slow strain-controlled axial-test apparatus in current use. The new critical state concept gives an edge to our decisions on the value of various pieces of existing test equipment.

All that we have written in this book has been concerned with saturated remoulded soil. Of course engineers need to test unsaturated soil, to test natural anisotropic or sensitive soil, and to test soil *in situ.* The new critical state concept enables us to separate effects that can be associated with isotropic behaviour from these special effects that are not predicted by the critical state models. The critical state concept gives a rational basis for design of new tests that explore aspects of behaviour about which little is known at present.

10.4 Soil Deformation and Flow

The limiting equilibrium calculations that we have introduced in chapters 8 and 9 correspond to problems of the 'strength' of a soil body experiencing imposed *total* stress changes indicated by the arrows from B and D in Fig. 10.3(a). The arrow from B corresponds to a problem of *immediate* limiting equilibrium (such as that discussed in §8.7), and the arrow from D corresponds to a problem of *long-term* limiting equilibrium (such as that discussed in §8.8).

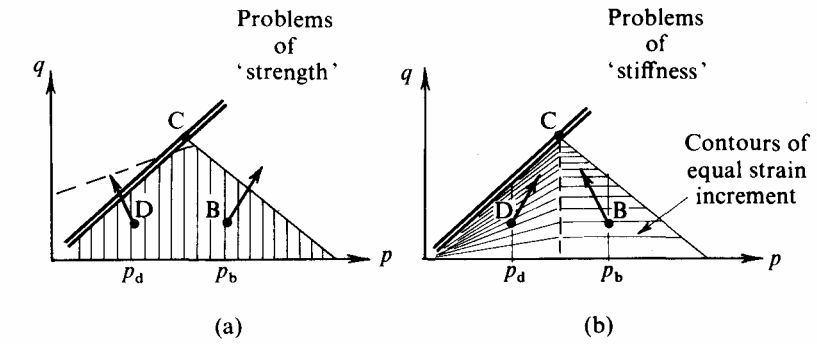

Fig. 10.3 Engineering Design Properties

However, we have not considered in this book a wide class of civil engineering design problems concerned with the 'stiffness' of a soil body. For example, in Fig. 10.3(b) the arrow of *effective* stress change from D might correspond to the distortion of firm ground beneath the base of a deep-bored cylinder foundation, and the arrow of *effective* stress change from B might correspond to the distortion of soft ground around a sheet-piled excavation. This type of design problem must become increasingly important in civil engineering practice, and it is clear that a better understanding of the stiffness of soil and its strain characteristics is required.

The critical state models that we have discussed in this book provide the basis for calculation of deformation in the rather special case of yielding of 'wet' soil. These models as they stand will not allow prediction of distortion for the loading of Fig. 10.3 because they are rigid for such loading, but research experiments and theoretical modifications to the models (for example, to allow recoverable distortion) do suggest the existence of 'contours' of equal distortion increments such as those shown in Fig. 10.3(b).

In addition to research experiments on axial-test specimens, a wide variety of other experiments on models and on other shapes of specimen is being conducted by us and our colleagues and by research workers in our own and in other laboratories. In reading reports of such research it is helpful to recall the differences between Figs. 10.3(a) and (b). Engineering design calculations at present concentrate on *strength:* as increasing skill is shown by designers so *stiffness* becomes a problem of increasing importance. Present research which explores the stiffness of apparently rigid soil bodies should prove to be of increasing importance to engineering designers as their skill in design increases.

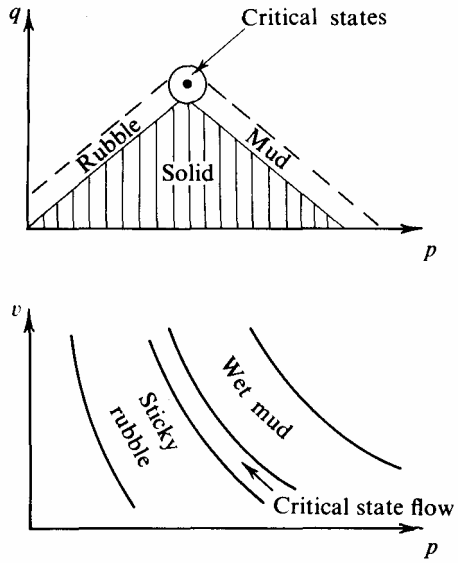

Fig. 10.4 Material Handling Properties

Throughout this book we have taken the civil engineer's viewpoint that it is, in general, undesirable for soil-material to move. We could equally well have taken the viewpoint of a material-handling engineer who wants powders and rubble to move freely. In Fig. 10.4 we repeat the (q, p) and (v, p) diagrams and indicate in a very crude manner the difference between states (p, v, q) in which the material (a) oozes as wet mud, (b) slips as a rubble of blocks (that stick to each other with an adhesion that depends on the pressure between the blocks), and (c) flows in the critical states. Clearly there are others as well as the civil engineer who may profit from the concept of §1.8 that 'granular materials, if continuously distorted until they flow as a frictional fluid, will come into a well-defined critical state'.